Delta University Scientific Journal 5 (2022) 66-82

Delta University Scientific Journal

Journal home page: https://digitalcommons.aaru.edu.jo/dusj/

Efficient Implementation of MIMO FBMC/OQAM Scheme based on Block Spreading

Walid Aly Raslan[1], Member, IEEE, Mohamed Abdel-Azim Mohamed[2], and Heba Mohamed Abdel-Atty[3], Senior Member, IEEE.

[1]Assistant Professor, Electronics and Communication Engineering Department, Faculty of Engineering, Delta University for Science and Technology, Gamasa, Egypt.
[2]Professor of Electronics and Communication Engineering Department, Faculty of Engineering, Mansoura University Mansoura 35516, Egypt.
[3]Associate professor at Electrical Engineering Department, Faculty of Engineering, Port Said University, Port Said 42524, Egypt

Correspondence: [Walid A. Raslan.]; [Faculty of Engineering, Delta University for Science and Technology, Gamasa, Egypt.]; Tel [+201225841034]; Email : walid.raslan@ymail.com

ABSTRACT
Filter bank multicarrier (FBMC) was proposed as an alternative approach to cyclic prefix - orthogonal frequency division multiplexing (CP-OFDM). FBMC is considered a promising non-orthogonal waveform due to its very low out of band radiation and high spectral efficiency. Nevertheless, the orthogonality constraint for FBMC/OQAM is relaxed being limited only to the real field which causes intrinsic interference. The presence of this interference leads to incompatibility between some well-known multiple-input and multiple-output (MIMO) schemes and FBMC/ offset quadrature amplitude modulation (OQAM). From this perspective, we proposed in this paper an efficient implementation for FBMC/OQAM based on block spreading to restore the complex orthogonality to enable applying MIMO with FBMC/OQAM. The proposed scheme uses a discrete Haar transform (DHT) to enable low computational complexity. The performance of proposed approaches has been investigated and compared with CP-OFDM under three MIMO schemes, as space-time block coding (STBC) Alamuoti schemes, spatial multiplexing with zero-forcing (ZF), and maximum likelihood (ML) detection schemes. The simulation results show that the proposed schemes enable to apply of the MIMO schemes with FBMC with almost the same performance and complexity as CP-OFDM.

Keywords: *Filter bank multicarrier/ offset quadrature amplitude modulation; multiple-input and multiple-output; discrete Haar transform; space-time block coding; zero-forcing; maximum likelihood .*

1- Introduction

Next-generation wireless communication systems necessitate the improvement of wireless systems to meet the new requirements in next network scenarios such as ultra-reliable and low latency communications (URLLC), enhanced mobile broadband (eMBB), and massive machine-type communications (mMTC) (Popovski et al. 2018),(De Almeida et al. 2019). Since next-generation wireless networks promise to be the future telecommunications technology, there have several requirements. it is required that the next-generation wireless network waveform can achieve these requirements (Taheri et al. 2017). Indeed, the most commonly used modulation system for wireless networks is OFDM due to its high performance in frequency selective channels (Bingham 1990). OFDM uses a rectangular pulse shape. However, OFDM has serious problems in spectral efficiency (Chen et al. 2018) and significant limitations, such as (i) High out-of-band (OoB) radiation, which causes interference between the neighboring channels. (ii) A CP overhead reduces the spectral efficiency CP overhead, which causes a reduction

in spectral efficiency. (iii) The strict time synchronization to ensure the orthogonality, which requires stringent time and frequency synchronization to avoid frequency and timing offsets, that makes it not the most suitable waveform for all targeted application scenarios (Wunder 2016).

The devolvement in wireless systems requires rethinking of waveforms with better characteristics to meet new requirements (Çatak and Durak-Ata 2016; Demir et al. 2018). In this paper, we will focus on our work in FBMC which is considered a promising waveform while avoiding the drawbacks of the CP-OFDM (De Almeida et al. 2019; Chen et al. 2020; Demir et al. 2018; Santacruz et al. 2020). FBMC exploits the prototype filter for each subcarrier to separate between subchannels in the frequency domain, in which this prototype filter differs from the rectangular pulse that is used in OFDM (Farhang-Boroujeny 2011), (Cherubini, Eleftheriou, and Olcer 2003). FBMC constructs the orthogonality in the real part with imaginary interference which causes the intrinsic imaginary interference. This interference has a significant effect on channel estimation and compatibility with some MIMO schemes. This turns out to be even more problematic because this leads to requiring new methods to apply MIMO schemes and new channel estimation methods. Indeed, applying OFDM to MIMO channels is a simple statement, but the direct deployment of FBMC to MIMO channels is a non-trivial issue due to the intrinsic interference and omitted CP (Perez-Neira et al. 2016).

Several studies on different MIMO-FBMC schemes have recently been carried out. The authors in (Zakaria and Le Ruyet 2012) investigated the combination of OFDM/OQAM using the IOTA function and MIMO the authors found that Alamouti coding may be executed only when it has come with code division multiple access (CDMA), considering the two different pulse shapes IOTA and PHYDYAS. However, this method is very sensitive to time variations of the channel and requires high computational complexity.

Blockwise Alamouti systems were provided for the FBMC using the PHYDYAS prototype filter (Le, Moghaddamnia, and Peissig 2016; Renfors, Ihalainen, and Stitz 2010). In these arrangements, the transmitted symbols were coded in a time or frequency inversion frame structure. Hence, traditional Alamouti decoding could be used after FBMC demodulation to decoding the received symbols. These systems are simple to deploy and do not damage the FBMC data structure. However, serious degradation occurs in high-frequency selective channels because the channel frequency response should be flat on each subcarrier to maintain full diversity in the receiver.

Recent work in (Singh, Budhiraja, and Vasudevan 2019) investigates symbol-error-rate (SER) of the FBMC-OQAM based MIMO systems for the MMSE detection. Also, the channel and CFO effects have been considered in (Singh et al. 2018). In (Singh and Rani 2018), a new technique is investigated for the detection in MIMO-FBMC-OQAM systems called neighborhood detection based ZF-successive interference cancellation.

The authors in (Nissel, Blumenstein, and Rupp 2017; Nissel and Rupp 2016) introduced a very effective solution to recover complex orthogonality in FBMC by spreading data symbols in frequency or time. The spreading technique itself has not added more complexity since it depends on a Walsh Hadamard transform which is considered the multiplication-free scheme. The FBMC/OQAM system studied in these works (Nissel, Blumenstein, et al. 2017; Nissel and Rupp 2016) was evaluated based on the PHYDYAS prototype filter in the case of frequency spreading and the Hermite prototype filter in the case of time spreading.

Therefore, an important issue in the literature is the difficulty to apply some MIMO schemes due to FBMC imaginary interference. The proposed solutions in the literature were divided into two directions. First, they tried to treat this interference and reduce its effects which usually cause degradation in system performance or destroy orthogonality. The second direction is to restore the complex orthogonality which causes to increase complexity. So that, In our work, we will try to solve this issue depend on the second solution (restore complex orthogonality) by employing block spreading as in (Nissel, Blumenstein, et al. 2017; Nissel and Rupp 2016) based on DHT which offers low computational complexity.

The main contributions of this paper are proposed efficient block spreading techniques with FBMC/OQAM systems in both time and frequency to restore complex orthogonality, evaluated the performance of these approaches with well-known MIMO schemes as STBC Alamouti schemes and spatial multiplexing schemes, and verified the validation of these schemes by comparing their performance with CP-OFDM.

The rest of the paper has been organized as follows. Section 2 represents the basics of FBMC systems and MIMO-FBMC. Next, the proposed schemes are explained in section 3. Then, section 4 presents the simulation results and discussion. Finally, the paper is concluded in section 5.

2- FBMC Systems

FBMC was introduced in (Siohan, Siclet, and Lacaille 2002), is namely FBMC/OQAM or staggered modulated multitoned (SMT), use the OQAM instead of QAM which the real and imaginary components are staggered by T0/2. This scheme is promising techniques which can relax the orthogonality condition for real symbol only. Also, it has better spectral efficiency than OFDM while it doesn't need CP insertion (Sabeti, Saeedi-Sourck, and Omidi 2015).

2.1. FBMC/OQAM Transmpultiplexer Scheme

Figure 1 shows the TMUX structure of the FBMC/OQAM system (Viholainen et al. 2009). In TMUX, the prototype filter is the primary element in the scheme since all filters are obtained from this prototype filter. As shown in Figure 1, the transmitter includes two main processes which are OQAM pre-processing, synthesis filter bank (SFB) since the receiver main processes are analysis filter bank (AFB) and OQAM post-processing. In the SFB, the $x_{m,n}$ is upsampled by factor M/2. The filtration process is applied to each subcarrier using a shifted version of the prototype filter gm[k] to obtain the transmitted signal. The discrete-Time description of a transmitted FBMC signal can be described as

$$s[k] = \sum_{n=-\infty}^{+\infty} \sum_{m=0}^{M-1} x_{m,n} g_m[k], \tag{1}$$

and the transmitted prototype filter as

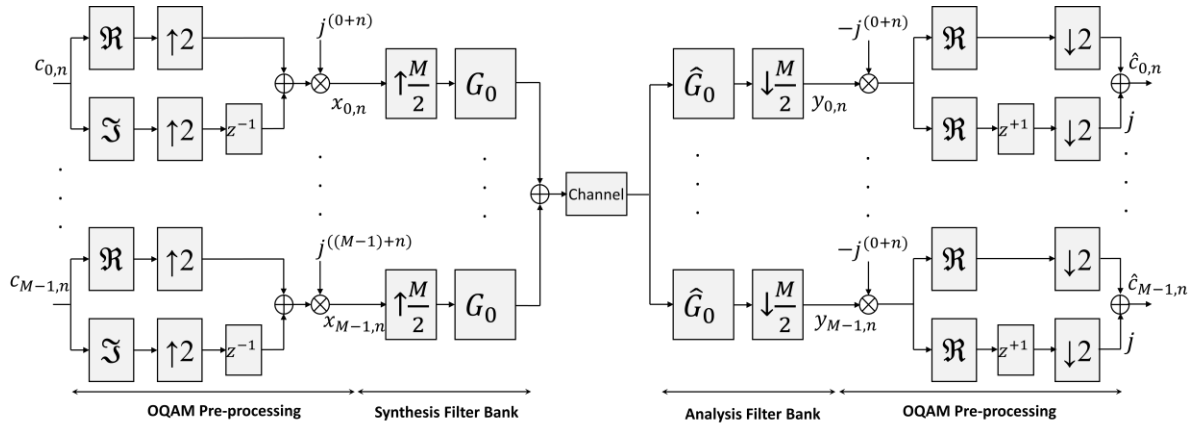

Figure 1: The TMUX scheme for FBMC/OQAM transceiver (Viholainen et al. 2009).The transmitted symbol $x_{m,n}$ is the combination of real and imaginary components.

$$g_{m,n}[k] = g\left[k - \frac{nM}{2}\right] e^{j\frac{2\pi}{M}m(k-\frac{L_p-1}{2})} e^{j\phi_{m,n}}. \tag{2}$$

where $g_{m,n}[k]$ is the prototype filter (Bellanger 2001; Viholainen et al. 2009).

In the AFB, the demodulated symbol $y_{m,n}$ can be obtained by the projection of the received signal $r[k]$ on the corresponding receive filter $\hat{g}_m[k]$ as

$$y_{m,n} = \langle s, \hat{g}_{m,n} \rangle = \sum_{k=-\infty}^{+\infty} r[k] \hat{g}_m[k - nM/2], \tag{3}$$

where

$$\hat{g}_m[k] = g_m^*[k] = e^{-j\frac{2\pi}{M}mk} g[k] \tag{4}$$

Then, the received signal will be

$$y_{m,n} = \sum_{n'=-\infty}^{+\infty} \sum_{m'=0}^{M-1} x_{m',\mathrm{n}'}[\mathrm{k}] \sum_{k=-\infty}^{+\infty} g_{m',n'}[k] g_{m,n}^*[k], \tag{5}$$

Since the FBMC/OQAM supports the property of orthogonality in the real domain only. So the prototype filters should satisfy the following condition.

$$\Re\left\{ \sum_{k=-\infty}^{+\infty} g_{m',n'}[k] g_{m,n}^*[k] \right\} = \delta_{m,m'}\delta_{n,n'} \tag{6}$$

where δ is the Kronecker delta. Therefore, the equation (5) can be rearranged to

$$y_{m,n} = x_{m,n} + \underbrace{\sum_{(m',\mathrm{n}')\neq(m,n)} x_{m',n'} \sum_{k=-\infty}^{+\infty} g_{m',n'}[k] g_{m,n}^*[k]}_{I_{m,n}} \tag{7}$$

where $I_{m,n}$ is the FBMC/OQAM intrinsic interference. while the transmitted data symbols satisfy the orthogonality condition in real symbols, then the $I_{m,n}$ term is a purely imaginary interference, $I_{m,n}$ =j$u_{m,n}$, where the $u_{m,n}$ is real. Thus, equation (7) will be:

$$y_{m,n} = x_{m,n} + ju_{m,n} \tag{8}$$

where $u_{m,n}$ is the intrinsic interference, is the imaginary interference and is described as (Taheri et al. 2017). Consequently, this intrinsic interference depends on the prototype filter.

$$u_{m,n} = \sum_{(\bar{m},\bar{n})\neq(m,n)} x_{\bar{m},\bar{n}} \underbrace{g_{\bar{m}}[k - \bar{n}M/2] \hat{g}_m[k - nM/2]}_{\langle p \rangle_{\bar{m},\bar{n}}^{m,n}} \tag{9}$$

The TMUX response, $\langle p \rangle_{\bar{m},\bar{n}}^{m,n}$, depend on the prototype filter. After channel equalization, the complex received symbol $\hat{c}_{m,n}$ cab be obtained from $y_{m,n}$ in the OQAM post-processing as in Figure 1.

2.2. FBMC/OQAM with MIMO systems

As OFDM and other multicarrier systems, FBMC is typically associated with MIMO systems via the Vertical Bell Labs Layered Space-Time (V-BLAST) transmitting scheme (Kofidis et al. 2013). Despite being possible to combine FBMC with other schemes, Since MIMO FBMC is a really interesting possible technique for the next generation of wireless communications systems. Indeed, applying OFDM to MIMO channels is a simple statement, but the direct deployment of FBMC to MIMO channels is a non-trivial issue due to the intrinsic interference and omitted CP (Kofidis et al. 2013).

In the case of a single antenna, if $x_{m,n}^j$ is the transmitted symbol, then the demodulated signal $y_{m,n}^i$is given by (Zakaria and Le Ruyet 2012):

$$y_{m,n}^i \approx h_{m,n}^{ij}(x_{m,n}^{\mathrm{j}} + ju_{m,n}^j) + \eta_{m,n}^i \tag{10}$$

where j is the index for the transmitted antenna and i for the received antenna. $h_{m,n}^{ij}$ presents the channel and $\eta_{m,n}^i$ is the noise part at the receiving antenna i, and $u_{m,n}^j$ is the intrinsic interference.

Therefore, when using N_t antennas to transmit N_t data symbols and using N_r antennas to receive the transmitted signals in the MIMO system, the received signal at the receiving antenna i can be expressed as:

$$r^{(i)} = \sum_{l=1}^{N_T} h^{(i,l)}[l] * s^{(l)} + \eta^{(i)}, \tag{11}$$

where $h[k, \ell]$ is the ℓ-th tap channel impulse response between j[th] transmitting and the i[th] receiving antenna. After passing through the FBMC analysis filter bank, the FBMC demodulated signal is described by (Zakaria and Le Ruyet 2012):

$$y_{m,n}^{(i)} = \sum_{i=1}^{N_r} h_{m,n}^{ij}(x_{m,n}^{i} + ju_{m,n}^{j}) + \eta_{m,n}^{j} \tag{12}$$

By assuming that each subchannel is flat and the channel coherence time is long enough to be greater than a transmission frame in an FBMC system, one can establish the following relationship between the received and transmitted symbols (Perez-Neira et al. 2016; Zakaria and Le Ruyet 2012):

$$y_{m,n} = H_m(x_{m,n} + ju_{m,n}) + \eta_{m,n}, \tag{13}$$

Then, the received signal matrix can be described as:

$$\underbrace{\begin{bmatrix} y_{m,n}^{1} \\ \vdots \\ y_{m,n}^{N_r} \end{bmatrix}}_{y_{m,n}} = \underbrace{\begin{bmatrix} h_{m,n}^{11} & \cdots & h_{m,n}^{1N_t} \\ \vdots & \ddots & \vdots \\ h_{m,n}^{N_r 1} & \cdots & h_{m,n}^{N_t N_r} \end{bmatrix}}_{H_{m,n}} \underbrace{\begin{bmatrix} x_{m,n}^{1} + ju_{m,n}^{1} \\ \vdots \\ x_{m,n}^{N_t} + ju_{m,n}^{N_t} \end{bmatrix}}_{x_{m,n}+ju_{m,n}} + \underbrace{\begin{bmatrix} \eta_{m,n}^{1} \\ \vdots \\ \eta_{m,n}^{N_r} \end{bmatrix}}_{\eta_{m,n}} \tag{14}$$

where $H_{m,n}$ represents the $(N_r \times N_t)$ channel frequency response (CFR) matrix. Since the equation (13) is classical per subcarrier representation of MIMO systems, there is a vast number of detection techniques that can be deployed to retrieve $x_{m,n}$ (Perez-Neira et al. 2016; Zakaria and Le Ruyet 2012).

2.3. MATRIX-BASED representation of FBMC/OQAM

In this section, we represent the FBMC/OQAM system model which is reviewed previously, in Matrix form for simplicity (Nissel, Schwarz, and Rupp 2017). The transmitted prototype filter can be defined by $\boldsymbol{G} \in \mathbb{C}^{1\times MN}$ matrix.

$$G = \begin{bmatrix} g_{1,1} & \cdots & g_{M,1} & g_{1,2} & \cdots & g_{M,N} \end{bmatrix} \tag{15}$$

and transmitted symbols $\boldsymbol{x} \in \mathbb{C}^{MN\times 1}$, are described as:

$$x = \begin{bmatrix} x_{1,1} & x_{2,1} & \dots & x_{\mathrm{M},1} & x_{1,2} & \dots & x_{\mathrm{M,N}} \end{bmatrix}^{T} \tag{16}$$

We can rewrite transmitted signal s(t) that is given in (2.1)

$$s = Gx \tag{17}$$

As in (3), the received symbols can be reformulated by

$$y = G^{H} r = G^{H} HGx + n \tag{18}$$

where $\boldsymbol{r} \in \mathbb{C}^{N\times 1}$ represents the received signal and $n \sim \mathcal{CN}(0, P_n G^H \mathrm{G})$ is the Gaussian distribution noise, with P_n the time white Gaussian noise power. Efficient Implementation of MIMO FBMC/OQAM using Spreading Techniques

3- Proposed MIMO FBMC/OQAM Approaches

In this section, we propose an efficient implementation of FBMC with MIMO based on block spreading. While the FBMC systems spread the symbols over time-frequency position, the block spreading technique has added the code dimension as the third dimension. This will make the symbols to be spread over several time slots or frequency positions instead of only one position which leads to more sensitivity to a high selective channel. We propose a two-block spreading scheme which one for spreading over time and the others for spreading over frequency. Also, the proposed scheme is extended to MIMO and employs the DHT to offer low computational complexity which have not a multiplication process only addition.

Our model is based on the idea of literature (Nissel, Blumenstein, et al. 2017; Nissel and Rupp 2016). However, we will use Haar matrices in the spreading process for enabling low complexity. As in (Nissel, Blumenstein, et al. 2017), the Balian-Low theorem has been satisfied by applying the orthogonality for real symbols only $x_{m,n} \in \mathbb{R}$, instead of the complex orthogonality, which leads to relax the orthogonality situation (Strohmer and Feichtinger 2012). If both time and frequency spacing reduced by 2, $T_0F = 1/2$ but for real-valued symbols, then complex symbols $T_0F = 1$. This frequency-time squeezing causes interference.

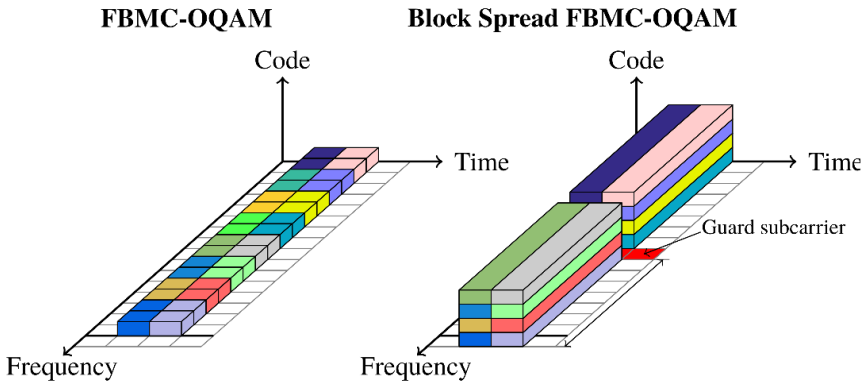

Figure 2: Conventional FBMC/OQAM transmission where only real symbols can be positioned Coded FBMC/OQAM transmission where complex symbols are spread over multiple frequency subcarriers. Different frequency blocks are separated by a guard subcarrier (Nissel, Blumenstein, et al. 2017).

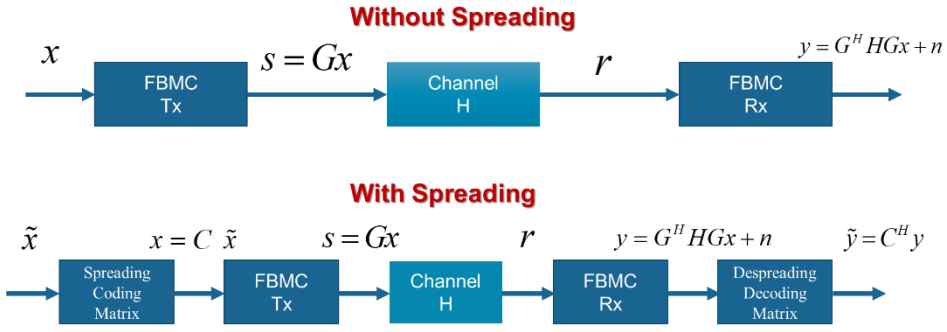

Figure 3: the block diagram of the proposed FBMC scheme compared with the conventional FBMC scheme.

Figure 2 illustrates the conventional and block spreading in frequency for FBMC transmission idea. Real-symbols can be transferred over a time-frequency rectangular position. The primary issue with FBMC is imaginary interference. This issue can be avoided by spreading data symbols over multiple time gird or several subcarriers, which enables the transmission of complex symbols with blocking of the imaginary interference.

Figure 3 shows the block diagram of the spreading FBMC scheme compared with the conventional FBMC scheme. The spreading technique is required the additional step in both transmitter and receiver for spreading and dispreading, respectively.

For block spreading, the spreading/coding matrix $C \in \mathbb{C}^{MN\times\frac{MN}{2}}$, is used to precode the complex symbols $\tilde{x} \in \mathbb{C}^{\frac{MN}{2}\times 1}$, so the transmitted data symbols $x \in \mathbb{C}^{MN\times 1}$ are obtained by

$$x = C\ \tilde{x} \tag{19}$$

and the received data symbols $\tilde{y}$ are produced by decoding the received symbols

$$\tilde{y} = C^H y \tag{20}$$

For the AWGN channel, the received prototype filter matrix in (18) (without spreading), assuming $= \boldsymbol{I_N}$, can be written as

$$\mathbf{y} = \mathbf{G}^H\mathbf{G}\mathbf{r} = \mathbf{D}\mathbf{x} + \mathbf{n} \tag{21}$$

where $\boldsymbol{D} = \boldsymbol{G^H G}$ is the transmission matrix and $n \sim \mathcal{CN}(0, P_n D)$ is random noise. Note that (21) shows a block of M subcarriers and N symbols transmission. To attain a required bandwidth and transmission time, some of these blocks should be concatenated in frequency and time.

With spreading, an equation (21) can be written as

$$\tilde{y} = C^H G^H G x = C^H D C\tilde{x} \tag{22}$$

To maintain the complex orthogonality, the spreading matrix C must satisfy the following situation.

$$C^H D C = I \tag{23}$$

Off-diagonal elements will represent imaginary interference, the identity matrix will be $\Re\{D\} = I_{MN}$ only by taking the real part. By taking an eigenvalue decomposition of the transmission matrix $\boldsymbol{D} = \boldsymbol{G^H G} = \boldsymbol{U\lambda U^H}$ with the unitary matrix U, A spreading matrix $C \in \mathbb{R}^{MN\times\frac{MN}{2}}$, that satisfies the condition in (23), can be as

$$C = U\begin{bmatrix} \lambda_1^{-1/2} & 0 & 0 \\ 0 & \ddots & 0 \\ 0 & 0 & \lambda_{MN/2}^{-1/2} \\ 0 & \cdots & 0 \\ \vdots & \ddots & \vdots \\ 0 & \cdots & 0 \end{bmatrix} \tag{24}$$

Where λ_i represents the i-the eigenvalue of $\boldsymbol{D}$. For $M \to \infty$ and $N \to \infty$, **D** has just $MN/2$ eigenvalues with a value equal to 2. Therefore, only $MN/2$ complex data symbols are transmitted, which is equal to transmit MN real data symbols.

This condition (23) can be satisfied by applying an eigenvalue decomposition, but this approach will be a high number of computational and complexity. To enable low complexity, we use $M \times M$ Haar matrix and data symbols spreading over $M/2$ column vectors of a matrix. The optimal coding matrix can be achieved under the condition of $M \to \infty$ and $N \to \infty$, and (24) with applying the water-filing algorithm as described in (Telatar 2008). Once, it is impossible to achieve this condition where the coding matrix limited to size $MN \times \frac{MN}{2}$, the coding matrix can be suboptimal for large numbers of M and N. In addition, the big advantage of DHT spreading is no multiplications required but only additions, so that the complexity is increased slightly, a drawback is the length of the coding must be a power of two. This makes it hard to integrate within systems, but when a system is built from scratch, it has almost no effect (Zakaria and Le Ruyet 2012).

Then, the coding matrix in (24) and prototype filter are applied to the symbols so that the transmitted signal can be expressed as

$$s = GC\tilde{x} = \tilde{G}\tilde{x}, \tag{25}$$

where

$$\tilde{G} = GC = \begin{bmatrix} \tilde{g}_1 & \tilde{g}_2 & \cdots & \tilde{g}_{MN/2} \end{bmatrix} \tag{26}$$

3.1. Block Spreading in Time

The coding matrix for spreading in time can be provided by $\boldsymbol{C_1} \in \mathbb{R}^{N\times\frac{N}{2}}$ and $\boldsymbol{C_2} \in \mathbb{R}^{N\times\frac{N}{2}}$ where one has to switch between C_1 and C_2 for neighboring subcarrier. The spreading matrix can be found by taking the DHT matrix as in (Wang 2012). The DHT matrix $\boldsymbol{\mathcal{H}} \in \mathbb{R}^{N\times N}$ for $N = 4$ as example:

$$\mathcal{H}_2^T = \frac{1}{2}\begin{bmatrix} 1 & 1 & 1 & 1 \\ 1 & 1 & -1 & -1 \\ \sqrt{2} & -\sqrt{2} & 0 & 0 \\ 0 & 0 & \sqrt{2} & -\sqrt{2} \end{bmatrix} \tag{27}$$

Then, the two coding matrices $\boldsymbol{C_1}$,$\boldsymbol{C_2}$ can be calculated as follow:

$$\begin{aligned} \left[\mathbf{C}_1\right]_{n,r} = \left[\mathcal{H}\right]_{n,2r-1} \text{ and } \left[\mathbf{C}_2\right]_{n,r} = \left[\mathcal{H}\right]_{n,2r} \\ \text{for } \; n = 1\ldots N;\, r = 1\ldots\frac{N}{2}. \end{aligned} \tag{28}$$

The coding matrix $\boldsymbol{C} \in \mathbb{R}^{MN\times\frac{MN}{2}}$, can be calculated as in (Nissel and Rupp 2016)

$$C = C_1 \otimes I_{M/2} \otimes \begin{bmatrix} 1 & 0 \\ 0 & 0 \end{bmatrix} + C_2 \otimes I_{M/2} \otimes \begin{bmatrix} 0 & 0 \\ 0 & 1 \end{bmatrix} \tag{29}$$

Next, the overall spreading matrix, as N=4 example, will be

$$\mathbf{C} = \frac{1}{2}\begin{bmatrix} 1 & 0 & \sqrt{2} & 0 \\ 0 & 1 & 0 & 0 \\ 1 & 0 & -\sqrt{2} & 0 \\ 0 & 1 & 0 & 0 \\ 1 & 0 & 0 & 0 \\ 0 & -1 & 0 & \sqrt{2} \\ 1 & 0 & 0 & 0 \\ 0 & -1 & 0 & -\sqrt{2} \end{bmatrix} \tag{30}$$

The orthogonality condition (23) can be satisfied by (30). Assuming the length of block N time slots and the number of blocks is three $\boldsymbol{x_1}, \boldsymbol{x_2}, and\ \boldsymbol{x_3}$, and corresponding prototype filter with spreading $\widetilde{\boldsymbol{G}}_1, \widetilde{\boldsymbol{G}}_2, and\ \widetilde{\boldsymbol{G}}_3$. Then, the transmitted signal can be written as

$$s = [\tilde{G}_1 \quad \tilde{G}_2 \quad \tilde{G}_3]\begin{bmatrix} x_1 \\ x_2 \\ x_3 \end{bmatrix} \tag{31}$$

Where each transmitted block $x_i \in \mathbb{C}^{MN\times 1}$. Then, By neglecting noise, the received data symbols of block 2 can be calculated by

$$\begin{aligned} \tilde{y}_2 &= C^H G_2^H s \\ &= C^H G_2^H G_1 \tilde{x}_1 + C^H G_2^H G_2 \tilde{x}_2 + C^H G_2^H G_3 \tilde{x}_3 \\ &= \tilde{x}_2 + \underbrace{C^H G_2^H G_1 \tilde{x}_1 + C^H G_2^H G_3 \tilde{x}_3}_{\text{interference}} \end{aligned} \tag{32}$$

3.2. Block Spreading in Frequency

The flat frequency channel for a length of spreading and flat time within one symbol is assumed to enable a low complexity equalizer. We apply a guard subcarrier to separate between frequency blocks as in (Nissel, Blumenstein, et al. 2017). We can rewrite the coding matrix **C** to satisfy the condition as (23) (as a spread over frequency only) (Nissel, Blumenstein, et al. 2017):

$$C = I_N \otimes C_0 \tag{33}$$

The frequency spreading matrix for a one-time slot is described by $C_0 \in \mathbb{R}^{N\times\frac{N}{2}}$. As in the time spreading, The spreading matrix can be found by taking the DHT matrix as in (Wang 2012). The DHT matrix $\boldsymbol{\mathcal{H}} \in \mathbb{R}^{\boldsymbol{N\times N}}$, we can get the coding matrix C_0:

$$\left[C_0\right]_{n,r} = \left[\mathcal{H}\right]_{n,2r} \quad for \quad n = 1\ldots N; r = 1\ldots\frac{N}{2}. \tag{34}$$

Then, the coding matrix can be calculated in the same manner as in time spreading in the previous subsection.

4- Simulation Results and Discussion

We exploit the block spreading in time or frequency to restore the complex orthogonality of the FBMC/OQAM system, as the Alamouti coding scheme requires the complex orthogonality property. Our MIMO FBMC/OQAM scheme applies not only to the Alamouti scheme but also to well-known MIMO methods that can be combined with our model such as the spatial multiplexing scheme. In this section, we verify the validity of our proposed schemes in terms of PSD, SIR, and, the BER under various channel models. Furthermore, we compare our results with other prototype pulse shaping filters and with CP-OFDM as a benchmark to prove the validity of our models in MIMO.

4.1. Power Spectral Density (PSD)

The good localization of the spectrum of the transmitted signal is the primary benefit of the FBMC technique. The PSD is defined as the content of power in the signal versus the frequency range. The FBMC signal has a coefficient of the prototype filters as one of its components. Therefore, OoB emissions can be reduced by selecting the appropriate prototype filter. The PSD can be calculated as in (Abdel-Atty, Raslan, and Khalil 2020).

Simulations are performed to check the PSDs and make comparisons of the PSD efficiency of the proposed prototype filters which were proposed in (Abdel-Atty et al. 2020) after spreading. In this simulation, we set the parameters as follows: i) subcarrier spacing F (15 kHz, same as LTE); ii) number of subcarriers M=24; iii) number of FBMC symbols N=105; iv) modulation order of 16 QAM; v) block frequency spreading with spreading length = 32; and vi) OFDM as in (Nissel, Schwarz, et al. 2017). We only consider the transmitted date on the first subcarrier (before spreading) because the PSD is calculated from the summation of all subcarrier that represents the frequency-shifted version of the first one. The simulated PSDs are acquired by inserting arbitrary symbols to FBMC/OQAM and then evaluating the transmitted signal PSDs for each prototype filter.

Figure 4 illustrates the PSDs of the OFDM and coded FBMC/OQAM systems. FBMC/OQAM achieve good spectral characteristics relative to CP-OFDM, in which the rectangular pulse that is used in OFDM, causing high OoB radiations, and we observe that the power of FBMC/OQAM in the OoB region is lower than that of CP-OFDM. By comparing Coded FBMC/OQAM (Figure 4) with conventional FBMC/OQAM in (Abdel-Atty et al. 2020), we can notice that PSD in Figure 4 is the same as the PSD in (Abdel-Atty et al. 2020) with a few ripples.

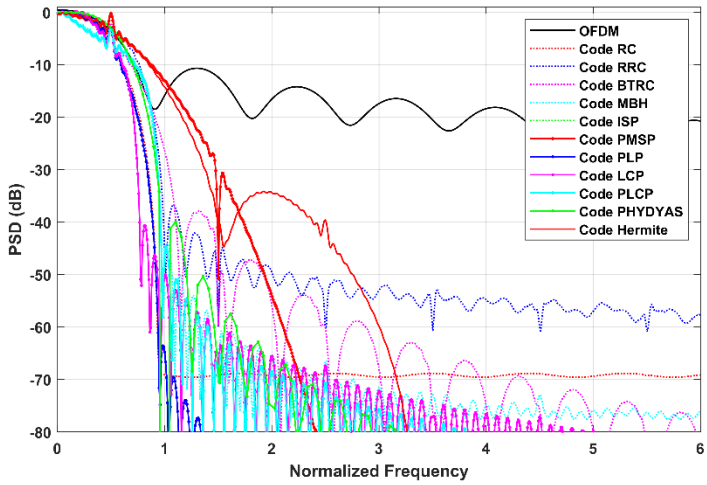

Figure 4: PSD of Coded FBMC vs. Normalized frequency f/F (applying the block frequency spreading), the unique spectral properties of FBMC are still maintained.

To conclude, A DHT transform can decrease computational complexity (Wang 2012). Hence, $\log_2(N) - 1$ extra additions or subtractions are needed at the transmitter for each complex symbol, and $\log_2(N)$ extra additions or subtractions are also needed at the receiver. The DHT approach's only minor drawback is that the length of spreading should be a power of two. Furthermore, apart from a few tiny ripples are added due to spreading, DHT spreading has almost no impact on the PSD (see Figure 4), so FBMC's superior spectral properties are maintained.

4.2. Signal-to-Interference Ratio (SIR)

First, the impact of a Rayleigh fading channel is investigated, we neglect the noise in the frequency spreading scheme, where the first term (32) represents the signal power while the second and third term the undesired interference. The SIR of block 2 can thus be expressed:

$$SIR_2 = \frac{MN/2}{\left\|C^H G_2^H G_1 C\right\|_F^2 + \left\|C^H G_2^H G_3 C\right\|_F^2} \tag{35}$$

Simulation results for the SIR over spreading length M lengths for each considered prototype filter can be found in Figure 5. While the parameters of the simulation are summarized in Table 1.

Table 1: SIR Simulation Parameters

PARAMETERS	VALUE
Modulation Order	16
Number of Symbols (N)	32
Spreading Length (M)	2 to 128
Subcarrier Spacing (F)	15 kHz
Carrier Frequency (fc)	2.5 GHz
Number of guard subcarriers	1 (spreading in frequency)
Channel models (Anon 2017)	Short delay spread of 10 ns.
	Pedestrian A (delay spread of 46 ns).
	Vehicular A (delay spread of 370 ns).

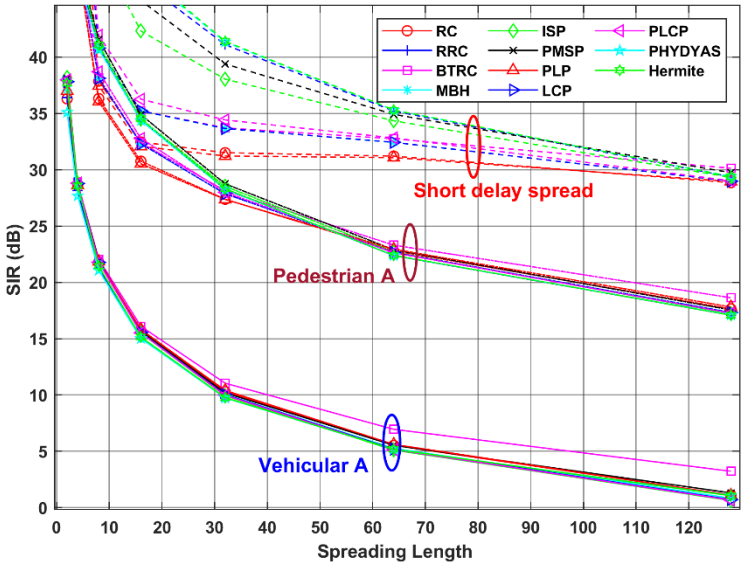

Figure 5: SIR performance for FBMC proposed prototype filters using different spreading lengths under three different channel delay spread (10 ns, 46 ns Pedestrian A channel, and 370 ns Vehicular A).

Figure 5 shows how the SIR depends on the spreading length. We can observe that the interference increases with increasing the length of spreading. However, the spectral efficiency increases with increasing spreading length. For the 10ns delay case, spreading can be easy with a high spreading length of 128. For the Pedestrian A case, to achieve the target SIR, the spreading length should be no more than 64. For Vehicular A, the frequency spreading technique suffers from high interference that leads to low SIR. Also, only for a high delay spread (Vehicular A), the higher the spreading length, the higher the spectral efficiency. However, a high spreading length also leads to high interference caused by the channel. Due to the high overhead needed for enough SIR, our approach is inadequate. Instead, could be employed the multi-tap equalization at the cost of complexity.

4.3. Bit Error Rate (BER)

Here, we check the validity of the described block frequency spreading approach with the benefit of restoring complex orthogonality, which is expected to enable usage of all MIMO schemes used in OFDM, for different MIMO schemes by simulation. The simulation parameters are the same as those in Table 2. The simulation is run with 1024 Monte Carlo repetitions.

4.3.1. Block Spreading in Frequency

A 2×1 Alamouti STBC scheme, which achieves full diversity at rate one , is considered in Figure 6, Figure 7, and Figure 8 show the performance of the FBMC 2×2 spatial multiplexing MIMO for ZF detection and ML detection, respectively. In 2×2 spatial multiplexing, independent bitstreams at both antennas are simultaneously transmitted. The transmitted symbols are detected at the receiver either by ZF equalization, which enhances the noise or by ML detection , which may increase the complexity.

We assume the Gaussian noise distribution and perfect knowledge of the channel. Note that ML detection in conventional FBMC is not viable because, owing to imaginary interference, too many variables have to be calculated. These figures also give a comparison of OFDM and FBMC using the proposed prototype filters based on block frequency spreading.

Figure 6, Figure 7, and Figure 8 show that the frequency spreading FBMC achieves approximately the same performance as CP-OFDM for only the Pedestrian A channel, but, the added benefit of higher spectral characteristics. Under Vehicular A, we observe degradation in error performance. This is because of the channel-induced interference which leads to a SIR of approximately 9 dB, see Figure 5. To gain robustness, we might need to reduce the spreading length. Also, we can observe high deviations between CP-OFDM and FBMC. Due to the lack of a CP, FBMC tends to be more susceptible to long delay spread channels. CP-OFDM outperforms FBMC in the Vehicular channel. Finally, the results show that all prototype filters verify the validity of the block frequency spreading approach in FBMC with different MIMO schemes.

Table 2: BER Simulation Parameters.

PARAMETERS	VALUE	
	TIME-SPREADING	FREQUENCY SPREADING
Modulation Order	16	
Number of Symbols (N)	32	
Number of Subcarriers (M)	512	
Subcarrier Spacing (F)	15 kHz	
Carrier Frequency (fc)	2.5 GHz	
Number of guard subcarriers	-	1
Number of guard symbols	3	-
Spreading length	16-time slots	32 subcarrier
Number of blocks	2	16
Total number (symbols or subcarriers)	35 symbols	528 subcarrier
Channel models (Anon 2017)	Pedestrian A (RMS delay spread of 46 ns).	
	Vehicular A (RMS delay spread of 370 ns).	
MIMO	2×1 Alamouti STBC scheme	
	2×2 spatial multiplexing with ZF detection	
	2×2 spatial multiplexing with ML detection	

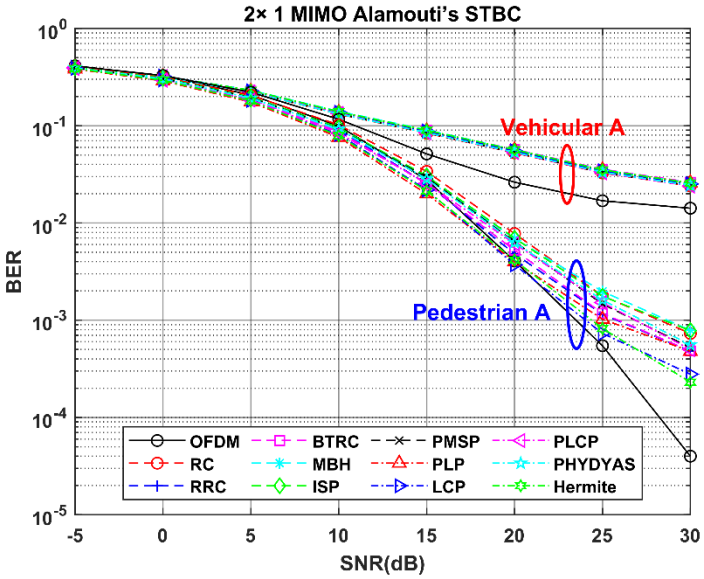

Figure 6: BER performance comparison between CP-OFDM and block frequency spreading FBMC using different prototype filters in 2 × 1 Alamouti's STBC scheme over the Pedestrian A and Vehicular A channel.

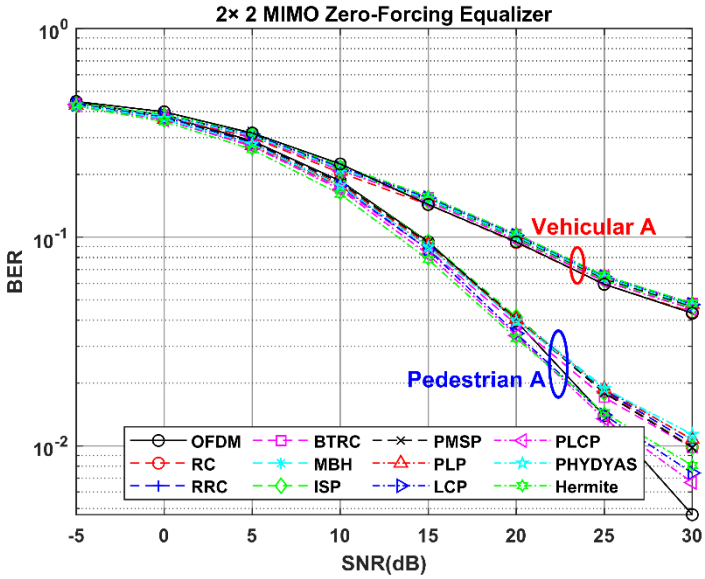

Figure 7: BER performance comparison between CP-OFDM and block frequency spreading FBMC using proposed prototype filters in 2 × 2 MIMO scheme using ZF detection over the Pedestrian A and Vehicular A channel.

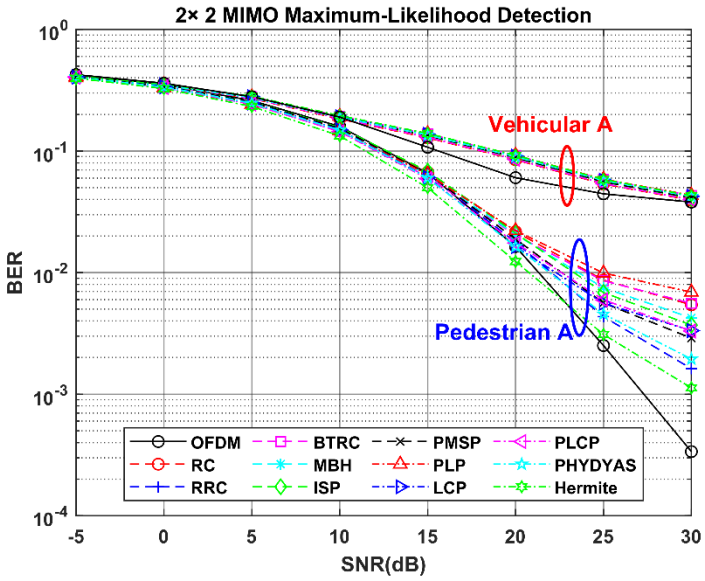

Figure 8: BER performance comparison between CP-OFDM and block frequency spreading FBMC using proposed prototype filters in 2 × 2 MIMO scheme using ML detection over the Pedestrian A and Vehicular A channel.

4.3.2. Block Spreading in Time

As previously explained, The main reason for spreading symbols over several time slots is to enable MIMO transmissions in FBMC with approximately the same MIMO complexity as in OFDM. Here, we spread in time instead of frequency. Also, we apply the same MIMO schemes described in frequency spreading and verify the validity of the block time spreading approach. The simulation parameters are chosen as shown in Table 2.

Figure 9, Figure 10, and Figure 11 show that FBMC achieves approximately the same performance as CP-OFDM. However, we can observe that the higher delay spread channel (Vehicular A) cause degradation in error performance, for both CP-OFDM and FBMC, than the lower delay spread channel (Pedestrian A). Additionally,

all prototype filters verify the validity of the block time spreading approach in FBMC with different MIMO schemes.

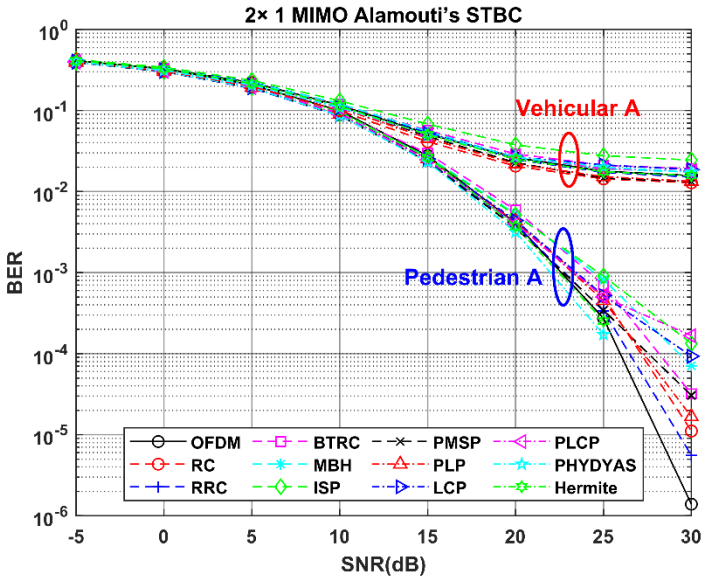

Figure 9: BER performance comparison between CP-OFDM and block time spreading FBMC using proposed prototype filters in 2 × 1 Alamouti's STBC scheme over the Pedestrian A and Vehicular A channel model.

Compared to the frequency spreading approach to the time-spreading approach, the two approaches provide approximately the same performance in time-variant channels. However, it can be seen that the CP-OFDM is more robust to long delay spread channels in the frequency spreading approach due to the presence of the CP

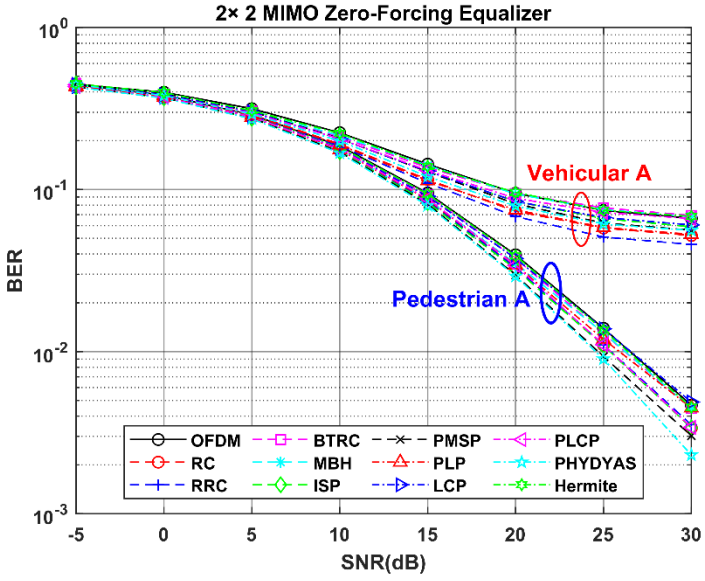

Figure 10: BER performance comparison between CP-OFDM and block time spreading FBMC using proposed prototype filters in 2 × 2 MIMO scheme using ZF detection over the Pedestrian A and Vehicular A channel model.

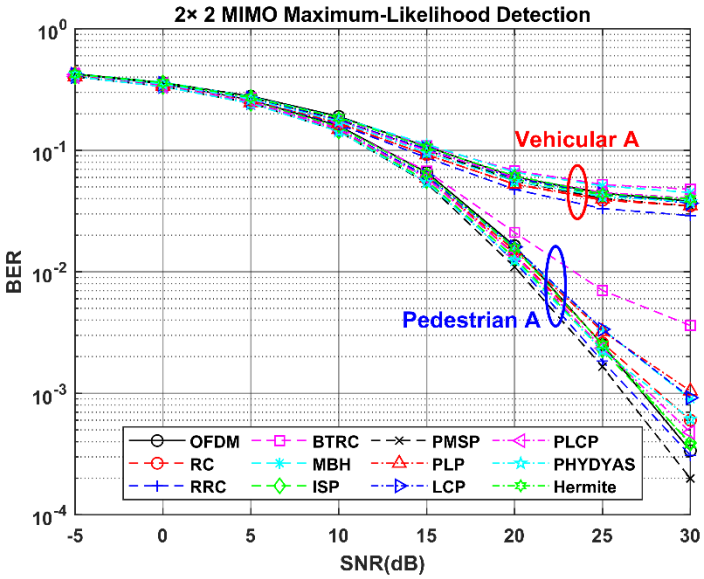

Figure 11: BER performance comparison between CP-OFDM and block time spreading FBMC using proposed prototype filters in 2 × 2 MIMO scheme using ML detection over the Pedestrian A and Vehicular A channel model.

5- Conclusions

We enhanced the structure of the MIMO FBMC/OQAM systems by spreading data symbols over time or frequency to restore complex orthogonality. We proposed this efficient approach in this paper. Based on this model we stated that the block spreading FBMC/OQAM allows us to straightforwardly employ all methods known in MIMO-OFDM such as spatial multiplexing and STBC Alamuoti schemes to apply in MIMO-FBMC. The coding matrix which satisfies the complex orthogonality on FBMC systems has been derived. Although the analytical spreading matrix required high computational complexity, a more practical solution is based on DHT because it requires almost no additional complexity. Furthermore, the usage of guard symbols is employed, this feature helped us to improve SIR because it reduces the interferences between blocks. The proposed system was examined and compared with OFDM in moderate and highly frequency selective channel scenarios, According to the results, the block spreading has almost no impact on the PSD. Additionally, the proposed spreading schemes in time or frequency with three MIMO techniques, 2×1 Alamouti STBC, 2×2 SM with ZF detection, and 2×2 SM with ML detection, compared with CP-OFDM can obtain almost the same performance in terms of the BER as CP-OFDM. However, FBMC still outperforms OFDM because of the much better spectral properties. These enhancements came at the cost of degradation in SIR only in case of high delay spread or Doppler spread channel. This can be explained by the channel induced interference. Such interference, however, does not influence low to medium delay spread or Doppler spread. Furthermore, we have shown that all proposed prototype filters verify the validity of the block time and frequency spreading approach with different MIMO schemes. In essence, the restoring of complex orthogonality by spreading in time or frequency and applying the DHT matrix enable to apply of the MIMO schemes for FBMC with almost the same performance and complexity as CP-OFDM.

References

Abdel-Atty, Heba M., Walid A. Raslan, and Abeer T. Khalil. 2020. “Evaluation and Analysis of FBMC/OQAM Systems Based on Pulse Shaping Filters.” *IEEE Access* 8:55750–72.

De Almeida, Ivo Bizon Franco, Luciano Leonel Mendes, Joel J. P. C. Rodrigues, and Mauro A. A. Da Cruz. 2019. “5G Waveforms for IoT Applications.” *IEEE Communications Surveys and Tutorials* 21(3):2554–67.

Anon. 2017. “Guidelines for Evaluation of Radio Interface Technologies for IMT-2020.” *Report ITU-R M.2412-0* 0.

Bellanger, M. G. 2001. “Specification and Design of a Prototype Filter for Filter Bank Based Multicarrier

Transmission." Pp. 2417–20 in *2001 IEEE International Conference on Acoustics, Speech, and Signal Processing. Proceedings (Cat. No.01CH37221)*. Salt Lake City, UT, USA.

Bingham, J. A. C. 1990. "Multicarrier Modulation for Data Transmission: An Idea Whose Time Has Come." *IEEE Communications Magazine* 28(5):5–14.

Çatak, Evren and Lütfiye Durak-Ata. 2016. "Waveform Design Considerations for 5G Wireless Networks." P. 13 in *Towards 5G Wireless Networks*. Vol. i. InTechOpen.

Chen, Da, Yuan Tian, Daiming Qu, and Tao Jiang. 2018. "OQAM-OFDM for Wireless Communications in Future Internet of Things: A Survey on Key Technologies and Challenges." *IEEE Internet of Things Journal* 5(5):3788–3809.

Chen, Yun, Wenfeng Liu, Zhiang Niu, Zhongxiu Feng, Qiwei Hu, and Tao Jiang. 2020. "Pervasive Intelligent Endogenous 6G Wireless Systems: Prospects, Theories and Key Technologies." *Digital Communications and Networks* (May).

Cherubini, Giovanni, Evangelos Eleftheriou, and Sedat Olcer. 2003. "Filtered Multitone Modulation for VDSL." *Conference Record / IEEE Global Telecommunications Conference* 2:1139–44.

Demir, Ali Fatih, Mohamed H. Elkourdi, Mostafa Ibrahim, and Huseyin Arslan. 2018. "Waveform Design for 5G and Beyond." Pp. 51–76 in *5G Networks: Fundamental Requirements, Enabling Technologies, and Operations Management*. Wiley-IEEE Press.

Farhang-Boroujeny, Behrouz. 2011. "OFDM Versus Filter Bank Multicarrier." *IEEE SIGNAL PROCESSING MAGAZINE* 28(3):92–112.

Kofidis, Eleftherios, Dimitrios Katselis, Athanasios Rontogiannis, and Sergios Theodoridis. 2013. "Preamble-Based Channel Estimation in OFDM/OQAM Systems: A Review." *Signal Processing* 93(7):2038–54.

Le, C., S. Moghaddamnia, and J. Peissig. 2016. "On the Performance of Alamouti Scheme in 2 x 2 MIMO-FBMC Systems." Pp. 1–6 in *ICOF 2016; 19th International Conference on OFDM and Frequency Domain Techniques*. Essen, Germany: VDE.

Nissel, Ronald, Jiri Blumenstein, and Markus Rupp. 2017. "Block Frequency Spreading: A Method for Low-Complexity MIMO in FBMC-OQAM." Pp. 1–5 in *IEEE Workshop on Signal Processing Advances in Wireless Communications, SPAWC*. Vols. 2017-July.

Nissel, Ronald and Markus Rupp. 2016. "Enabling Low-Complexity MIMO in FBMC-OQAM." Pp. 1–6 in *2016 IEEE Globecom Workshops, GC Wkshps 2016 - Proceedings*. Vol. 1.

Nissel, Ronald, Stefan Schwarz, and Markus Rupp. 2017. "Filter Bank Multicarrier Modulation Schemes for Future Mobile Communications." *IEEE Journal on Selected Areas in Communications* 35(8):1768–82.

Perez-Neira, Ana I., Marius Caus, Rostom Zakaria, Didier Le Ruyet, Eleftherios Kofidis, Martin Haardt, Xavier Mestre, and Yao Cheng. 2016. "MIMO Signal Processing in Offset-QAM Based Filter Bank Multicarrier Systems." *IEEE Transactions on Signal Processing* 64(21):5733–62.

Popovski, Petar, Kasper Floe Trillingsgaard, Osvaldo Simeone, Giuseppe Durisi, and Giuseppe Durisi Petar Popovski, Kasper F. Trillingsgaard, Osvaldo Simeone. 2018. "5G Wireless Network Slicing for EMBB, URLLC, and MMTC: A Communication-Theoretic View." *IEEE Access* 6(648382):55765–79.

Renfors, Markku, Tero Ihalainen, and Tobias Hidalgo Stitz. 2010. "A Block-Alamouti Scheme for Filter Bank Based Multicarrier Transmission." *2010 European Wireless Conference, EW 2010* (1):1031–37.

Sabeti, Parna, Hamid Saeedi-Sourck, and Mohamad Javad Omidi. 2015. "Low-Complexity CFO Correction of Frequency-Spreading SMT in Uplink of Multicarrier Multiple Access Networks." *ICEE 2015 - Proceedings of the 23rd Iranian Conference on Electrical Engineering* 10:410–15.

Santacruz, Javier Pérez, Simon Rommel, Ulf Johannsen, Antonio Jurado-Navas, and Idelfonso Tafur Monroy. 2020. "Candidate Waveforms for ARoF in beyond 5G." *Applied Sciences (Switzerland)* 10(11):1–16.

Singh, Prem, Rohit Budhiraja, and K. Vasudevan. 2019. "SER Analysis of MMSE Combining for MIMO FBMC-OQAM Systems with Imperfect CSI." *IEEE Communications Letters* 23(2):226–29.

Singh, Prem and Bagadi Usha Rani. 2018. "Neighbourhood Detection-Based ZF-V-BLAST Architecture for

MIMO-FBMC-OQAM Systems." *2018 IEEE Global Communications Conference (GLOBECOM)* 1–6.

Singh, Prem, Ekant Sharma, K. Vasudevan, and Rohit Budhiraja. 2018. "CFO and Channel Estimation for Frequency Selective MIMO-FBMC/OQAM Systems." *IEEE Wireless Communications Letters* 7(5):844–47.

Siohan, Pierre, Cyrille Siclet, and Nicolas Lacaille. 2002. "Analysis and Design of OFDM/OQAM Systems Based on Filterbank Theory." *IEEE Transactions on Signal Processing* 50(5):1170–83.

Strohmer, Thomas and Hans G. Feichtinger. 2012. *Gabor Analysis and Algorithms (Applied and Numerical Harmonic Analysis)*. New York, NY, USA: Springer.

Taheri, Sohail, Mir Ghoraishi, Pei Xiao, and Lei Zhang. 2017. "Efficient Implementation of Filter Bank Multicarrier Systems Using Circular Fast Convolution." *IEEE Access* 5:2855–69.

Telatar, Emre. 2008. "Capacity of Multi-Antenna Gaussian Channels." *European Transactions on Telecommunications* 10(6):585–95.

Viholainen, Ari, Tero Ihalainen, Tobias Hidalgo Stitz, Markku Renfors, and Maurice Bellanger. 2009. "Prototype Filter Design for Filter Bank Based Multicarrier Transmission." Pp. 1359–63 in *European Signal Processing Conference*. IEEE.

Wang, Ruye. 2012. *Introduction to Orthogonal Transforms: With Applications in Data Processing and Analysis*. Illustrate. Cambridge University Press.

Wunder, G. 2016. "5GNOW D1.6 v1.0 White Paper." *5GNOW_D1.6_v1.0*.

Zakaria, Rostom and Didier Le Ruyet. 2012. "A Novel Filter-Bank Multicarrier Scheme to Mitigate the Intrinsic Interference: Application to MIMO Systems." *IEEE Transactions on Wireless Communications* 11(3):1112–23.